Available online at www.sciencedirect.com
ScienceDirect
Bioorganic Chemistry 34 (2006) 235–247
BIOORGANIC CHEMISTRY
www.elsevier.com/locate/bioorg

# DNA sequence-directed assembly of two peptide bioconjugates

M. Thompson *

*Department of Chemistry, Michigan Technological University, 1400 Townsend Dr., Houghton, MI 49931, USA*

Received 9 March 2006
Available online 2 August 2006

**Abstract**

Peptide bioconjugates combine the molecular recognition features of the polypeptide from a DNA-binding protein and the DNA-sensitive fluorescence of an intercalating dye. Here, DNA template-directed assembly of two bioconjugate probes was examined by steady-state fluorescence resonance energy transfer and time-resolved single photon counting. The Förster critical distance was determined to be approximately 26 Å for the oxazole yellow and thiazole orange donor–acceptor pair. The efficiency of energy transfer for two bioconjugates was a function of the number of intervening base pairs between two DNA cognate sites. These probes were sufficiently sensitive to detect sequence dependent curvature and polypeptide induced bending of the DNA. Molecular probes capable of examining spatial aspects of protein complexes at promoter sites could yield important information about the early events in transcription initiation.


*Keywords:* Thiazole orange; Oxazole yellow; Bioconjugate; DNA-binding protein; Protein–DNA interactions; Fluorescence resonance energy transfer (FRET)

## 1. Introduction

All known transcription initiation events involve multiple proteins that self-assemble into pre-arranged configurations based on chemical and structural features. For protein–DNA interactions, the sequence of the DNA acts as a template that selects the

* Fax: +1 906 487 2061.
*E-mail address:* mthomps@mtu.edu.

0045-2068/$ - see front matter © 2006 Elsevier Inc. All rights reserved.
doi:10.1016/j.bioorg.2006.06.001

identity and coordinates the assembly of multiple proteins. For example, DNA assembly-templates contain upstream regulatory elements, such as promoters, that facilitate the spatial organization of transcription factors. In many cases, these proteins bind DNA at distant sites and bend the DNA to form hetero- or homodimers [1]. Only then are such higher-order structures able to recruit and prime the transcriptional machinery. Consequently, mutations in the promoter region that affect the distance between protein binding sites can prevent the formation of these higher-order protein–DNA structures and adversely affect mRNA synthesis [2].

Molecular recognition events in protein–DNA interactions are central to many fundamental biological processes involved in regulating gene function. A growing number of studies are using fluorescence approaches and developing novel *in vitro* [3,4] and *in vivo* [5,6] fluorescent probes to understand the factors that drive site-specificity, localization, and detailed characteristics of biomolecular assembly. Molecular probes capable of examining the temporal and spatial aspects of higher order assembly at promoter sites could yield important information about the early events in transcription initiation.

Peptide-intercalator bioconjugates are fluorescent probes composed of a polypeptide from a DNA-binding protein and an asymmetric cyanine dye. In previous work, the thiazole orange-Tc3 transposase (TOTC3) and the oxazole yellow-Hin recombinase (YOHIN) bioconjugates revealed the dye moiety was only able to intercalate DNA and emit a strong fluorescence signal when the polypeptide was bound with high affinity to its native cognate site [7,8]. Fluorescence and electrophoretic analysis of these bioconjugates show that the DNA recognition features of the polypeptide control the ability of the dye to interact with DNA under physiological conditions [9]. In effect, the polypeptide moiety acts as a targeting element and the fluorophore acts as a reporter group. Such molecular probes have affinities and specificities, which exceed DNA-binding domains through the action of the attached intercalating dye, which anchors the bound peptide to the DNA. In the bound state of these bioconjugates, the dye associates with the dsDNA and fluoresces, but is essentially non-fluorescent in the unbound form. Peptide-intercalator bioconjugates have been shown to be highly sensitive probes of DNA sequence in single molecule [10] and ensemble fluorescence studies [8], and represent a new technology to study protein–DNA recognition features, targeting events, and spatial organization.

The intercalating dyes used here have the ability to report their binding state because they have the useful photophysical property of a quantum yield 3–4 orders of magnitude higher when intercalated into DNA compared to the unbound state. The monomeric thiazole orange (TO) has a fluorescence enhancement of approximately 3000 upon binding RNA [11]. It was postulated that this enhancement was due to a change in the relative orientation of the two heterocycles from skewed to coplanar upon intercalation. This characteristic feature of the cyanine family of dyes is exploited by the peptide bioconjugates which are fluorescent when DNA-bound and effectively invisible when not bound.

Prior work using a histone bioconjugate revealed important information about the assembly of histone proteins and DNA into nucleosomal structures [3]. A bioconjugate composed of thiazole orange and a single zinc finger from the glucocorticoid receptor protein was used to understand how the protein is able to discriminate the subtle differences between glucocorticoid and estrogen response elements [9]. In this work, two bioconjugates have been designed using different combinations of DNA recognition polypeptides and cyanine dyes to generate an acceptor–donor pair for fluorescence resonance energy transfer (FRET) analysis. The objective is to assess their utility in examining higher-order

assembly of protein–DNA complexes. Self-assembling systems, such as these could make useful probes for studying multi-protein assembly dynamics at promoter sites.

## 2. Materials and methods

### 2.1. Materials

Lepidine, 5-bromovaleric acid, 3-methylbenzothiazole-2-thione, 2-mercaptobenzoxazole, *para*-methyltoluenesulfonate, iodomethane, dipotassium carbonate, acetone, dichloromethane, anhydrous ethanol, and triethylamine were purchased from Aldrich (Milwaukee, WI) and used without further purification, except dioxane, which was distilled prior to use. F-moc amino acids and peptide synthesis reagents were purchased from Advanced Chemtech (Louisville, KY). The F-moc-Lys (Mtt)-OH was purchased from Anaspec (San Jose, CA).

### 2.2. Instrumentation

The peptide-bioconjugates were synthesized on a 9050 peptide synthesizer (Millipore, Bedford, MA). Purification of each bioconjugate was performed using high performance liquid chromatography (HPLC) and characterization was performed by matrix-assisted laser desorption ionization-time of flight (MALDI-TOF) mass spectrometry using α-cyanohydroxycinnamic acid. Absorbance measurements were made on a Cary V spectrophotometer (Varian Instruments, Palo Alto, CA). Steady-state fluorescence measurements were performed on a Quantamaster-6/2003 Spectrofluorometer in T-format, with a 75 W xenon lamp and analyzed with Felix32 Fluorescence Analysis Software (PTI, Canada). Fluorescence lifetime measurements were made using the time-correlated single photon counting method. The fundamental output from a Spectra Physics Tsunami laser was doubled by a Spectra Physics Model 3980 frequency doubler and pulse selector. The excitation rate was 4 MHz, pulse width 2 ps, average power *ca.* 1.1 W. A microchannel plate photomultiplier (Hamamatsu R2809U-11) was used to detect the fluorescence emission after passing the emission through a polarizer set at the magic angle with respect to excitation and through a single grating monochromator. The instrument response time was *ca.* 60 ps (Full Width at Half Maximum), as verified by scattering from Ludox AS-40. The spectrometer was controlled by software based on a Lab View program from National Instruments.

### 2.3. Bioconjugate peptide synthesis, purification and characterization

The cyanine dyes coupled to the DNA-binding regions were synthesized as described previously [7,9]. Dye-peptide bioconjugates were synthesized on PAL-PEG-PS resin by automated solid-phase peptide synthesis using F-moc chemistry. The bioconjugates were purified by RP-HPLC on a Zorbax $C_8$ column (9.4 mm × 25 cm) using a water (0.1% TFA)–acetonitrile (0.1% TFA) gradient. Identities of the bioconjugates were confirmed by amino acid analysis and MALDI-TOF mass spectrometry. Stock solution concentrations of the conjugated peptides were determined spectrophotometrically from the extinction coefficients of $\varepsilon_{479\ nm} = 40{,}500\ M^{-1}\ cm^{-1}$ for YOHIN and $\varepsilon_{503\ nm} = 50{,}800\ M^{-1}\ cm^{-1}$ for TOTC3 [7,8]. The primary sequences of the polypeptides derived from the Tc3

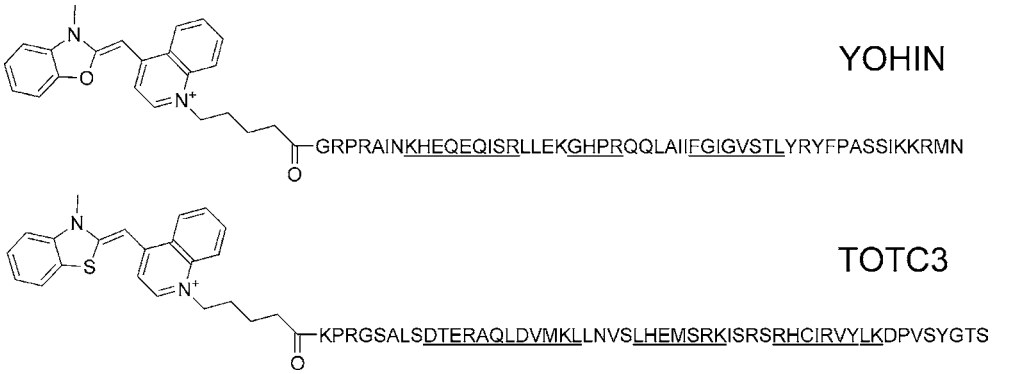


Fig. 1. Amino acid sequence of the dye-peptide bioconjugates. The oxazole yellow-Hin recombinase (YOHIN) and, the thiazole orange-Tc3 transposase (TOTC3) bioconjugate sequences are shown. The HIN polypeptide is derived from residues 139 to 190 of the native Hin recombinase and the TC3 polypeptide is derived from residues 202 to 253 of the native Tc3 transposase. The structures of the cyanine dyes are attached at the N-terminal amino acid are shown. The underlined residues are those having α-helical secondary structure.

transposase and Hin recombinase, as well as the position of cyanine dye incorporation are shown in Fig. 1.

### 2.4. DNA sample preparation

All oligonucleotides used here were synthesized on a DNA synthesizer using phosphoramidite chemistry and purified on a 12% denaturing polyacrylamide gel. Bands were cut out and recovered by soaking the crushed gel pieces in 100 mM Tris (pH 8.0) 100 mM NaCl buffer for 4–6 h. Extractions were combined and the urea and salts removed by spin filtration or size exclusion chromatography using Sephadex G-15. Concentrations for purified single stranded oligonucleotides were calculated using the nearest neighbor method [12]. Single DNA strands were annealed with one molar equivalent of the appropriate complementary strand. The oligonucleotides used in this study are 40-mers containing the native cognate sites for both the Tc3 transposase (TC3 ) and Hin recombinase (HIN) with three separation distances shown in Fig. 2.

### 2.5. Steady-state FRET measurements

Steady-state spectra and energy transfer efficiency determinations were performed at 100 nM of the indicated duplex DNA and 100 nM of the indicated bioconjugate using a

H8T : 5'-GCGCTCTTATCAAAACGCAGTCTATAGGACCCCCGCTCAC-3'

H12T: 5'-GTCGTCTTATCAAAACGCAGTCAGTCTATAGGACCCCCGC-3'

H16T: 5'-TCTTATCAAAACGCAGATCGTCAGTCTATCGGACCCCCGC-3'

HIN TC3

Fig. 2. The three oligonucleotide sequences used in these studies. The native DNA-sequences (underlined) for the Hin recombinase (HIN) and Tc3 transposase (TC3) DNA-binding domains have been incorporated into the DNA-template at three separation distances. H8T, H12T, and H16T have 8, 12, and 16 intervening bases that separate the HIN and TC3 cognate sites.

glass cuvette with 1 cm pathlength. Measurements were made at an excitation wavelength of 460 nm. The excitation is set at an absorption wavelength where YOHIN (donor) absorbs and minimizes contributions to the emission spectra by direct excitation of the TOTC3 (acceptor). The emission wavelength used to quantify donor quenching was 510 nm. The sample was titrated with acceptor over the concentration range of 0–150 nM. Steady-state energy transfer efficiency was evaluated from the decrease in donor emission after subtracting contributions from direct excitation of the acceptor and correcting for dilution due to titration with TOTC3. A 20 mM Tris (pH 7.6), 100 mM NaCl buffer was used for all measurements.

### 2.6. Determination of spectral properties

Samples for determination of the quantum yield contained 50–500 nM bioconjugate in 20 mM Tris, (pH 7.6) 100 mM NaCl with 500 nM of the appropriate cognate DNA to ensure complete binding. Fluorescence quantum yields ($\Phi_F$) for these samples were determined relative to fluorescein in 0.1 M NaOH ($\Phi_F = 0.90$) by integration of corrected emission spectra [13,14]. Solutions used for fluorescence quantum yield determination for the bioconjugates were made to have the same absorbance (*ca.* 0.03) at absorbance maximum for each dye.

The efficiency of energy transfer was examined using both steady-state and time-resolved approaches. Fluorescence resonance energy transfer efficiency ($E$) is determined by steady-state fluorescence intensity changes of the donor in the absence and presence of the acceptor [15] can be used to determine energy transfer efficiency according to:

$$E = 1 - \left(\frac{I_{DA}}{I_D}\right) \tag{1}$$

where $I_D$ and $I_{DA}$ are the experimentally determined fluorescence intensities of the donor in the absence and presence of the acceptor, respectively ($I_{DA}$ was corrected to remove any contributions from direct excitation of the acceptor). Both values are normalized to the same donor concentration. Efficiency of energy transfer is related to the distance ($r$) between dyes by the method discussed by Clegg [16]:

$$E = \frac{1}{1 + (r/R_o)^6} \tag{2}$$

Here, the Förster distance ($R_o$), which is defined as the distance where the rate of energy transfer to the acceptor equals the rate of donor fluorescence (or when the energy transfer efficiency equals 50%) is calculated from [17]:

$$R_o = 9.7 \times 10^3 \left(\frac{\kappa^2 \Phi_D J}{\eta^4}\right)^{1/6} \tag{3}$$

where the Förster distance is proportional to the orientation factor ($\kappa^2$) between donor and acceptor transition moments, the quantum yield of the donor in the absence of the acceptor ($\Phi_D$), the overlap integral ($J$), and the refractive index of the medium ($\eta$). Experiments with model systems have shown that the Förster theory is valid and applicable to distance determination, but the orientation factor has, until recently, remained a source of controversy. In many applications the fluorophore is tethered to the biomolecule by a

flexible linker arm, which provides enough dynamic averaging such that orientation factor ($\kappa$) does not significantly affect the accuracy of average distance measurements. Ultimately, unless the orientation between the two chromophores is explicitly known, the value of $\kappa^2 = 2/3$ is typically used for molecules randomly oriented with rapid tumbling [18]. Here, the cyanine dyes are in an unknown orientation relative to each other, but the fully intercalated dyes should not exhibit rapid orientational randomization. Therefore, a value of $\kappa^2 = 0.476$ was used because the dyes exhibit random static orientations on the timescale of the fluorescence lifetimes [19]. The index of refraction, $\eta$, is generally taken to be 1.33 for water at 22 °C [20] and speculated to be 1.4 for nucleic acids [19]. Since these dyes are intercalating dyes in a nucleotide containing solution, a value of 1.4 is used. It is unclear whether the energy transfer is occurring through space or through the DNA base stack. The overlap integral between the donor and the acceptor is given as:

$$J = \frac{\int F_{\mathrm{D}}(\lambda)\varepsilon_{\mathrm{A}}(\lambda)\lambda^4 \mathrm{d}\lambda}{\int F_{\mathrm{D}}(\lambda)\mathrm{d}\lambda} \tag{4}$$

where $F_{\mathrm{D}}$ is the peak-normalized fluorescence spectrum of the donor, $\varepsilon_{\mathrm{A}}$ is the molar absorption coefficient of the acceptor [21]. To solve Eqs. (3) and (4), it was necessary to determine the extinction coefficients and quantum yields of the conjugates as described above.

### 2.7. Time-correlated single-photon counting measurements

Lifetime analysis was performed using the same samples and buffers as described above for the steady-state measurements except that samples were composed of 100 nM YOHIN, 100 nM TOTC3, and 100 nM DNA in 20 mM Tris (pH 7.6), 100 mM NaCl buffer. Excitation of samples was at 450 nm and emission detection was at 510 nm. Fluorescence decays were analyzed by fitting to a sum of exponential decay terms convoluted with the measured instrument response function. This was done either at single measurement wavelengths or simultaneously to data taken at several emission wavelengths [22,23]. The values for $A_i$ and $\tau_i$ are solved using MATLAB by use of an application called ASUFIT, which deconvolutes the individual lifetime components and their respective amplitudes. The donor can be empirically modeled as a sum of exponentials:

$$I(t) = \sum A_i \mathrm{e}^{(-t/\tau_i)} \tag{5}$$

where $A_i$ and $\tau_i$ are amplitude and lifetime of the $i$th exponential. Subsequently, the average lifetime for a given fluorophore can be calculated from a weighted average of the measured lifetimes [15]:

$$\langle\tau\rangle = \frac{\sum A_i\tau_i}{\sum A_i} \tag{6}$$

Donor lifetimes in the presence and absence of acceptor can be used to calculate average energy transfer efficiency by the following equation:

$$E = 1 - \frac{\langle\tau_{\mathrm{DA}}\rangle}{\langle\tau_{\mathrm{D}}\rangle} \tag{7}$$

where $\langle\tau_{\mathrm{DA}}\rangle$ and $\langle\tau_{\mathrm{D}}\rangle$ are average donor lifetimes in the presence and absence of acceptor, respectively [24].

## 3. Results and discussion

### 3.1. Determination of spectral features

Initially, the photophysical properties of the peptide-linked fluorophores were characterized to assess their suitability for use in FRET assays. The bioconjugate probes YOHIN and TOTC3 each have a fluorescent dye attached to a DNA-targeting polypeptide (Fig. 1). The spectral features of the fluorophore change upon peptide linkage due to increased solvation [9]. The absorbance and fluorescence spectra of YOHIN and TOTC3 taken separately in the presence of DNA containing the H8T sequence clearly illustrates the spectral overlap of the oxazole yellow (YO) and the thiazole orange (TO) dyes of the conjugates (Fig. 3). The YOHIN has absorbance and fluorescence maxima at 490 and 508 nm, respectively. The TOTC3 has absorbance and fluorescence maxima at 510 and 529 nm, respectively. These two dyes show significant Förster overlap in the 495–520 nm range centered at approximately 509 nm.

The photophysical parameters required to calculate the Förster distance were determined for each of the bioconjugates. The parameters $J$ and $R_o$ were calculated from the absorbance and fluorescence spectra of the bioconjugates bound to their respective cognate sites to best represent the experimental conditions of the FRET studies. The overlap integral ($J$) is calculated from the quantum yield of the YO fluorophore from the YOHIN bioconjugate (0.37), which acts as the donor in this system and the extinction coefficient of the TO fluorophore from the TOTC3 (62,800 $M^{-1}$ $cm^{-1}$), which acts as the acceptor. The overlap integral $J(\lambda)$ was determined to be $5.1 \times 10^{-15}$ $cm^3$ $M^{-1}$ for the YO–TO pair when each dye is conjugated to each respective peptide. The calculated Förster distance for the YO–TO pair was 25.7 Å.

The resulting Förster distance is approximately half of that for more common FRET pairs, such as fluorescein and rhodamine, which have $R_o$ values of roughly 50 Å. The spec-

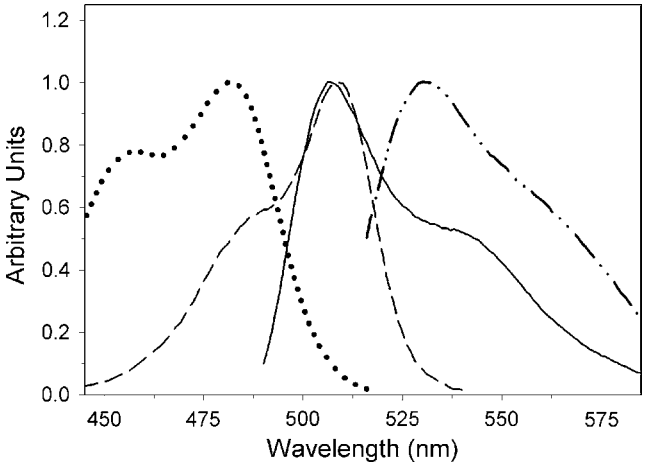


Fig. 3. Normalized absorbance and fluorescence spectra of DNA-bound YOHIN and TOTC3. The absorbance (···) and fluorescence (—) spectra for YOHIN (donor) and the absorbance (- - -) and fluorescence (–··–) spectra of TOTC3 (acceptor) are shown to illustrate the spectral overlap of the two bioconjugates.

tra of the dyes show a 20–25% decrease in the maximum absorbance upon peptide conjugation [7]. Previous studies indicate that cyanine dyes can adopt two modes of binding depending on concentration or temperature [25]. For the bioconjugates, the small adverse effect on the photophysical properties was attributed to steric constraints as the peptide that drives binding may force the dye to adopt a binding mode that has a lower quantum yield [7]. In spite of this modest adverse affect, these dyes are well suited to act as a FRET pair.

### 3.2. Steady-state FRET of bioconjugate probes

Steady-state fluorescence spectroscopy was used to examine the self-assembling YOHIN/TOTC3 system on DNA templates. The YOHIN and TOTC3 were incubated for 30 min with the indicated 40-mer of duplex DNA that contains the native cognate sites for both polypeptides at three separation distances. Representative spectra for the three DNA sequences incubated with 100 nM YOHIN and TOTC3 at a 1:1:1 ratio (dsDNA:YOHIN:TOTC3) show the changes in fluorescence with respect to separation of the binding sites (Fig. 4). The data were corrected to remove contributions to the observed spectra due to direct excitation of the TOTC3 (Section 2). The YOHIN bound to H8T in the absence of TOTC3 is shown for reference. The H16T sequence, which positions the two binding sites approximately 55 Å apart, shows a small quenching effect upon TOTC3 addition. The H12T sequence, which positions the two binding sites approximately 41 Å apart, shows the additive effect of TOTC3 addition and the decrease in direct emission from YOHIN due to energy transfer. The H8T sequence, which positions the two binding sites 27 Å apart, approximately equivalent to $R_o$ for the YO–TO dye pair, shows a significant effect upon TOTC3 addition.

The efficiency of energy transfer for all three cognate site separation distances was measured by pre-incubating 100 nM YOHIN with 100 nM of the appropriate dsDNA and examining the quenching induced by titration with TOTC3 (Fig. 5). TOTC3 was titrated into sample containing the YOHIN-DNA complex until no further change in fluorescence

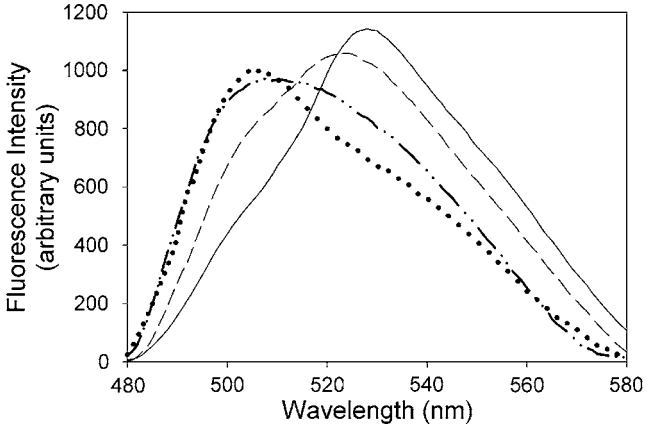


Fig. 4. Representative set of fluorescence spectra for each of the three DNA sequences in the presence of YOHIN and TOTC3. Concentrations of H8T (—), H12T (- - -), and H16T (–··–) DNA sequences and each bioconjugate are 100 nM. The emission spectra of DNA-bound YOHIN (···) in the absence of TOTC3 are shown for comparison.

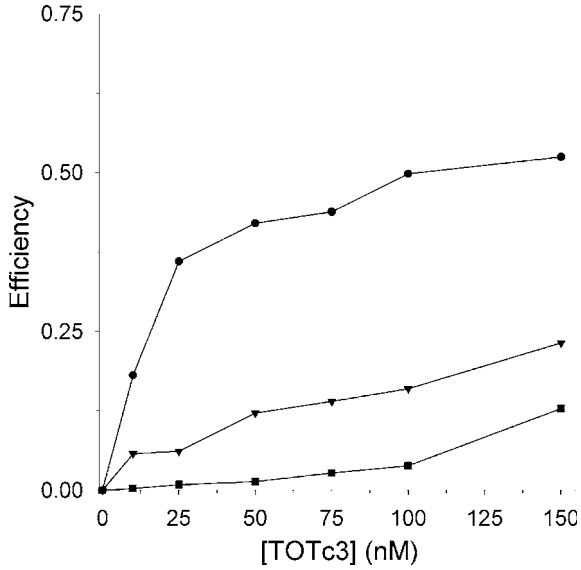


Fig. 5. Energy transfer efficiency. For each DNA sequence, 100 nM of the indicated sequence is pre-incubated with 100 nM YOHIN. The YOHIN-DNA complex is titrated with 0–150 nM TOTC3. The concentration of DNA and YOHIN was 100 nM for H8T (●), H12T (▼), and H16T (■) DNA sequences.

intensity occurred. The titration results clearly illustrate the dependence of YOHIN quenching efficiency with binding site separation distance over the course of the titration. The quenching at 1:1, YOHIN–TOTC3 was used to determine efficiency of energy transfer between the two conjugates bound to the three sequences. The corrected quenching efficiencies based on the integrated intensity of the YOHIN fluorescence spectra are 52% (H8T), 20% (H12T) and 5% (H16T).

Distance calculations from experimentally determined FRET efficiencies are evaluated by rearrangement of Eq. (2) to solve for $r$, the separation distance between donor and acceptor. From the steady-state fluorescence measurements, the distance dependence approximates the expected behavior if the dyes are being positioned at precise locations along the DNA-assembly template (Table 1). No decrease in fluorescence intensity was observed in controls titrated with unlabeled TC3 polypeptide (not conjugated to TO).

Table 1
Distance determination from FRET measurements

| | H8T | H12T | H16T |
|---|---|---|---|
| Distance[a] (calculated) | 27.2 | 40.8 | 54.4 |
| Steady-state | | | |
| Efficiency | 0.522 | 0.202 | 0.051 |
| Distance (observed) | 25.3 | 32.8 | 42.5 |
| Single-photon counting | | | |
| Efficiency | 0.470 | 0.245 | 0.078 |
| Distance (observed) | 26.5 | 31.5 | 40.7 |

[a] Distance between the HIN and TC3 binding sites for each DNA sequence assumes 3.4 Å per base.

The efficiencies of energy transfer as a function of distance were determined by monitoring the quenching of the YOHIN as it is titrated with the TOTC3 conjugate. Previous determinations of the dissociation equilibrium constants ($K_D$) for the bioconjugates were 10 nM for YOHIN and 15 nM for TOTC3 [8]. Using these $K_D$ values, greater than 95% of the YOHIN and TOTC3 should be bound to their cognate sites. At the concentrations used for these measurements, greater than 90% of the DNA templates are expected to have both bioconjugates bound and suggests that the efficiency of energy transferred represents a lower limit.

### 3.3. Single photon counting measurements

The fluorescence lifetimes were measured for the YOHIN and TOTC3 bioconjugates bound to each of the three DNA sequences (Fig. 2). The samples all had 100 nM each of donor, acceptor and the DNA template. The SPC measurements were performed in parallel with those described above for the steady-state fluorescence measurements. The data were corrected to remove contributions to the observed spectra due to instrument response (Section 2). The YOHIN bound to H8T in the absence of TOTC3 was previously examined and shown to have a lifetime of 1.92 ns [7]. The SPC traces for each of the three distances are shown in Fig. 6. The H16T sequence, which positions the HIN and TC3-binding sites the furthest distance apart, shows a small effect upon TOTC3 addition, whereas the H8T sequence, which positions the two binding sites in the closest proximity, shows the greatest effect upon TOTC3 addition.

The lifetime values were determined from a global fit of three sets of spectra for each sample taken over the emission wavelength range of 500–550 nm. Average lifetimes are calculated by summing the products of the emission lifetimes and their corresponding relative emission amplitudes for each bioconjugate donor–acceptor pair/dsDNA system. The average lifetime and the associated error are given for analyses using both bi- and tri-exponential decay fits for comparison (Table 2). The tri-exponential decay fit indicates a decrease in lifetime for YOHIN from 1.92 to 1.02 ns for the DNA having the two binding

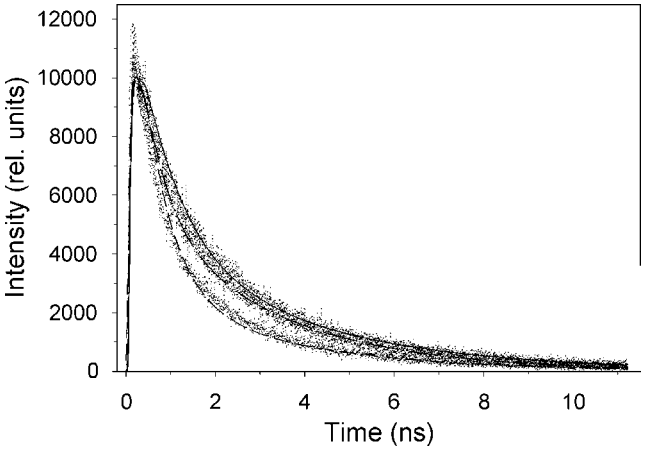


Fig. 6. Single photon counting trace. The exponential decays of each of the three DNA sequences in the presence of 100 nM YOHIN and TOTC3. The H8T (——), H12T (— —), and H16T (- - - - -) DNA sequences were at a concentration of 100 nM.

Table 2
Lifetimes[a] of YOHIN in the presence and absence of TOTc3 for each DNA sequence

| Sample | H8T | H12T | H16T |
|---|---|---|---|
| YOHIN | [0.58] 0.75 | — | — |
| ave $\tau$ | [0.42] 3.14 | | |
| $\chi^2$ | 1.92 | | |
| | 1.11 | | |
| [b]YOHIN + | [0.80] 0.40 | [0.55] 0.54 | [0.62] 0.88 |
| TOTC3 | [0.20] 3.13 | [0.45] 2.88 | [0.38] 3.52 |
| ave $\tau$ | 0.96 | 1.59 | 1.87 |
| $\chi^2$ | 1.68 | 1.24 | 1.20 |
| [c]YOHIN + | [0.45] 0.16 | [0.33] 0.21 | [0.33] 0.28 |
| TOTC3 | [0.34] 0.90 | [0.40] 1.19 | [0.40] 1.58 |
| | [0.21] 3.12 | [0.27] 3.41 | [0.27] 3.89 |
| ave $\tau$ | 1.02 | 1.46 | 1.78 |
| $\chi^2$ | 1.10 | 1.07 | 1.06 |

[a] Relative amplitudes of the emission decay fits are given as decimal fractions in brackets before the corresponding lifetime. Average emission lifetimes are calculated as the sum of the products of the emission lifetimes and their corresponding relative amplitudes.
[b] Bi-exponential decay fit.
[c] Tri-exponential decay fit.

sites in their closest position. The shortest component representing nearly half the YO population has a lifetime of 150 ps, consistent with a quenching mechanism. As the HIN and TC3-binding sites are separated, the lifetime increases to 1.5 and 1.8 ns, respectively. The YOHIN/TOTC3 system exhibits distance dependent changes in the lifetimes when bound to each of the three DNA sequences that follow the same trends observed in the steady-state FRET studies.

The average lifetime determined for the bioconjugates are 1.92 ns for YOHIN and 1.25 ns for TOTC3 when bound to their cognate site [7]. The average lifetimes were previously determined to be 2.22 and 1.33 ns for the unconjugated YO and TO, respectively [26]. The lifetimes of the cyanine dyes inherently have bi-exponential decays. The decrease in cyanine dye lifetime upon peptide conjugation was previously attributed to two DNA-binding modes of the dye [7,25]. The SPC studies reveal a complicated energy transfer mechanism between YOHIN and TOTC3 on the DNA templates that give rise to the observed tri-exponential decay kinetics. It is unclear whether this is due to alternate binding modes or intercalation induced changes in DNA structure.

### 3.4. FRET determination of separation distances

The HIN and TC3 cognate sites are separated by 8, 12, and 16 base pairs (Fig. 2). Assuming 3.4 Å per base, the expected distances are 27.2, 40.8, and 54.4 Å between the closest edges of the two cognate sites. Using Förster-based distance dependence, the distances between the two dyes localized by each respective DNA-binding domain were determined. Distances determined by averaging the steady-state and time-resolved methods were 25.9, 32.2, and 41.6 Å for H8T, H12T, and H16T, respectively. The shortest distance, which is approximately the same as the Förster distance, showed the closest match between expected and calculated values. As the distance increases, the difference between the expected and calculated distance also increases.

The difference between the experimentally determined and expected distances most likely reflects an induced curvature or distortion of the helical axis of the DNA by the bound conjugates. The Hin recombinase DNA-binding domain binds a cognate site that encompasses part of an A-tract. An A-tract seven bases in length is known to cause curvature in the absence of proteins of roughly 25° at a salt concentration of 100 mM [27]. *In vivo* this probably helps the Hin protein induce DNA bending for higher order complex formation. Similarly, the region flanking the TC3 cognate site has an AT stretch that was shown to have a protein induced bend of approximately 30° in the crystal structure [28]. The peptide-induced bending angles observed in each respective crystal structure and the overall DNA-bending determined experimentally will also be affected by the intercalated dye. Intercalating dyes are known to increase the DNA length by decreasing helical twist. TO was shown to cause a 20° decrease in the twist angle between adjacent base pairs upon intercalation [29]. In addition, dynamic fluctuations of the 40-mer may contribute to separation distances that deviate from values expected if DNA was strictly linear. It was previously shown using FRET that end to end distances in DNA are shorter than calculated due to sequence dependent bends and kinks, as well as global bending of the structure [19].

Alternatively, the separation distances can be interpreted from orientation factors that take into consideration the inherent twisting of B-DNA. Because both fluorophores intercalate perpendicular to the long axis of the DNA duplex and the location of one fluorophore is known relative to the other, the individual values for $\kappa^2$ for each separation distance can be estimated. The change in the relative orientation of the two dyes was based on an ideal B-DNA structure which has a twist of 34.5° per base pair and 10.5 base pairs per turn. Using the method of Dale et al. [30], which uses the relative orientation of the transition moments [31] for donor emission and acceptor excitation, $\kappa^2$ was determined to be 0.488, 0.793, and 0.615 for H8T, H12T, and H16T, respectively. This yields experimentally determined distances of 23.9, 33.0, and 41.1 Å for the 8, 12, and 16 base pair separation distances, respectively. Using both averaged and specific values for $\kappa^2$ confirms that experimentally determined separation distances are smaller than expected and consistent with DNA bending.

## 4. Conclusion

Peptide-dye bioconjugates are composed of a polypeptide from a DNA-binding protein and the dsDNA dependent fluorescence of an asymmetric cyanine dye. Here, DNA template-directed assembly of two probes was examined by fluorescence resonance energy transfer. The Förster critical distance was determined to be approximately 26 Å for the YOHIN and TOTC3 acceptor–donor pair. The efficiency of energy transfer decreased as the separation distance between binding sites increased. Interestingly, the probes proved to be sufficiently sensitive to detect sequence dependent curvature and polypeptide induced bending of the DNA. Molecular probes capable of examining the temporal and spatial aspects of higher order assembly at promoter sites could yield important information about the early events in transcription initiation.

## Acknowledgments

We thank Dr. Neal Woodbury for discussion and providing samples used in this study and Dr. Dan Brune for assistance with the peptide synthesizer.

## References

[1] C. Grandori, S.M. Cowley, L.P. James, R.N. Eisenman, Ann. Rev. Cell Dev. Biol. 16 (2000) 653–699.
[2] M. Pal, A.S. Ponticelli, D.S. Luse, Mol. Cell 19 (2005) 101–110.
[3] J. Babendure, P.A. Liddell, R. Bash, D. LoVullo, T.K. Schiefer, M. Williams, D.C. Daniel, M. Thompson, A.K.W. Taguchi, D. Lohr, N.W. Woodbury, Anal. Biochem. 317 (2003) 1–11.
[4] A.K. Eggleston, N.A. Rahim, S.C. Kowalczykowski, Nucleic Acids Res. 24 (1996) 1179–1186.
[5] M. Thompson, R.A. Haeusler, P.D. Good, D.R. Engelke, Science 302 (2003) 1399–1401.
[6] L. Wang, R.A. Haeusler, P.D. Good, M. Thompson, S. Nagar, D.R. Engelke, J. Biol. Chem. 280 (2005) 8637–8639.
[7] M. Thompson, Bioconj. Chem. 17 (2006) 507–513.
[8] M. Thompson, N.W. Woodbury, Biophys. J. 81 (2001) 1793–1804.
[9] M. Thompson, N.W. Woodbury, Biochemistry 39 (2000) 4327–4338.
[10] D.C. Daniel, M. Thompson, N.W. Woodbury, J. Phys. Chem. B 104 (2000) 1382–1390.
[11] L. Lee, C.-H. Chen, L. Chiu, Cytometry 7 (1986) 508–517.
[12] W. Rychlik, W. Spencer, R. Rhoads, Nucleic Acids Res. 18 (1990) 6409–6412.
[13] H. Ozaki, L.W. McLaughlin, Nucleic Acids Res. 20 (1992) 5205–5214.
[14] J.N. Demas, G.A. Crosby, J. Phys. Chem. B 75 (1971) 991–1024.
[15] W.S. Furey, C.M. Joyce, M.A. Osborne, D. Klenerman, J.A. Peliska, S. Balasabrumanian, Biochemistry 37 (1998).
[16] R.M. Clegg, Methods Enzymol. 211 (1992) 353–388.
[17] L. Stryer, Ann. Rev. Biochem. 47 (1978) 819–846.
[18] R.A. Cardullo, S. Agrawal, C. Flores, P.C. Zamecnik, D.E. Wolf, Proc. Natl. Acad. Sci. USA 85 (1988) 8790–8794.
[19] J. Wildeson, C. Murphy, Anal. Biochem. 284 (2000) 99–106.
[20] C.H. Cho, J. Urquidi, G.I. Gellene, G.W. Robinson, J. Chem. Phys. 114 (2001) 3157–3162.
[21] R.H. Fairclough, C.R. Cantor, Methods Enzymol. 48 (1978) 347–379.
[22] J. Peloquin, J. Williams, X. Lin, R. Alden, A. Taguchi, J. Allen, N. Woodbury, Biochemistry 33 (1994) 8089–8100.
[23] A. Taguchi, J. Stocker, R. Alden, T. Causgrove, J. Peloquin, S. Boxer, N. Woodbury, Biochemistry 31 (1992) 10345–10355.
[24] P. Wu, L. Brand, Anal. Biochem. 218 (1994) 1–13.
[25] J. Nygren, N. Svanvik, M. Kubista, Biopolymers 46 (1998) 39–51.
[26] T.L. Netzel, K. Nafisi, M. Zhao, J.R. Lenhard, I. Johnson, J. Phys. Chem. B. 99 (1995) 17936–17947.
[27] H.-S. Koo, D.M. Crothers, Proc. Natl. Acad. Sci. USA 85 (1988) 1763–1767.
[28] G.v. Pouderoyen, R.F. Ketting, A. Perrakis, R.H.A. Plasterk, T.K. Sixma, EMBO J. 16 (1997) 6044–6054.
[29] H. Spielmann, D. Wemmer, J. Jacobsen, Biochemistry 34 (1995) 8542–8553.
[30] R.E. Dale, J. Eisinger, W.E. Blumberg, Biophys. J. 26 (1979) 161–194.
[31] A. Larsson, C. Carlsson, M. Jonsson, Biopolymers 36 (1995) 153–167.